

Title: Fluoroalkylation of Dextromethorphan Improves CNS Exposure and Metabolic Stability

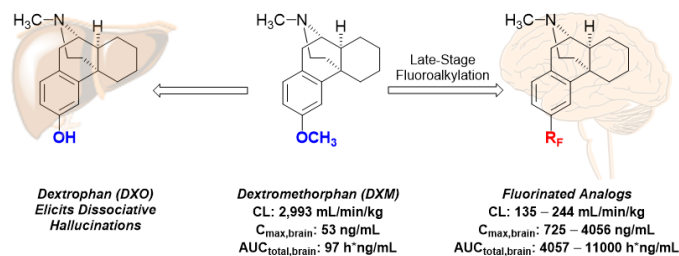
Authors' Names and Addresses: Jacob P. Sorrentino,[†] Ryan A. Altman^{#,*}

[†]Department of Medicinal Chemistry, The University of Kansas, Lawrence, Kansas 66045, United States

[#]Department of Medicinal Chemistry and Molecular Pharmacology and Department of Chemistry, Purdue University, West Lafayette, IN, 47906, United States

Corresponding author's email: raaltman@purdue.edu

TOC/Abstract Graphic



Abstract

Aryl-methyl ethers, while present in many bioactive compounds, are subject to rapid O-dealkylation that can generate bio-inactive or toxic metabolites. As an example, the cough suppressant dextromethorphan undergoes such a P450 mediated O-dealkylation to provide the psychoactive phenolic metabolite dextrophan. This metabolite antagonizes the NMDA receptor causing hallucinations, which encourages recreational abuse. To circumvent this undesired metabolism, we have designed, synthesized, and evaluated *in vitro* and *in vivo* new fluoroalkyl analogs of dextromethorphan that display improved pharmacokinetic profiles relative to dextromethorphan and related analogs currently in clinical trials. Specifically, the fluorinated analogs minimized metabolic degradation and increased CNS exposure relative to DXM *in vivo*. Ultimately, these fluorinated motifs might be applicable to other aryl-methyl ether containing compounds as a strategy to improve pharmacokinetic profiles.

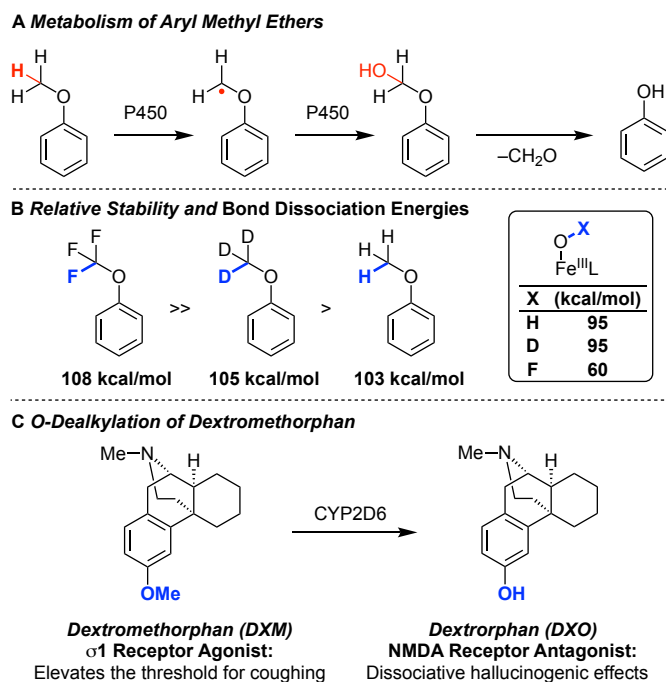
Keywords

Dextromethorphan, Fluoroalkylation, Aryl-Methyl Ether, O-Dealkylation

Introduction

Aryl methyl ethers are commonly encountered substructures in therapeutically relevant compounds, including natural products.^{1,2} Despite its prevalence, this motif is metabolically labile, as it can undergo extensive P-450 mediated metabolism via O-dealkylation to afford phenolic metabolites. In this process, the initial abstraction of a hydrogen atom generates a C-based radical, and subsequently a formyl hemi-acetal that ultimately hydrolyzes to reveal a phenol (Figure 1A). In some cases, this metabolism can be exploited as a prodrug strategy to improve distribution and pharmacokinetic properties (e.g. codeine and hydrocodone);³ however, in other cases, facile O-dealkylation can generate inactive or toxic phenolic metabolites that limit a drug's therapeutic utility.^{4,5} Thus, from a medicinal chemist's perspective, the ability to inhibit such unwanted metabolism, while retaining or improving a candidate's pharmacological profile, remains an essential goal.

Figure 1: (A) P450 Mediated Oxidation of Aryl Methyl Ethers. (B) Comparison of Bond Strengths. (C) Metabolism of DXM.

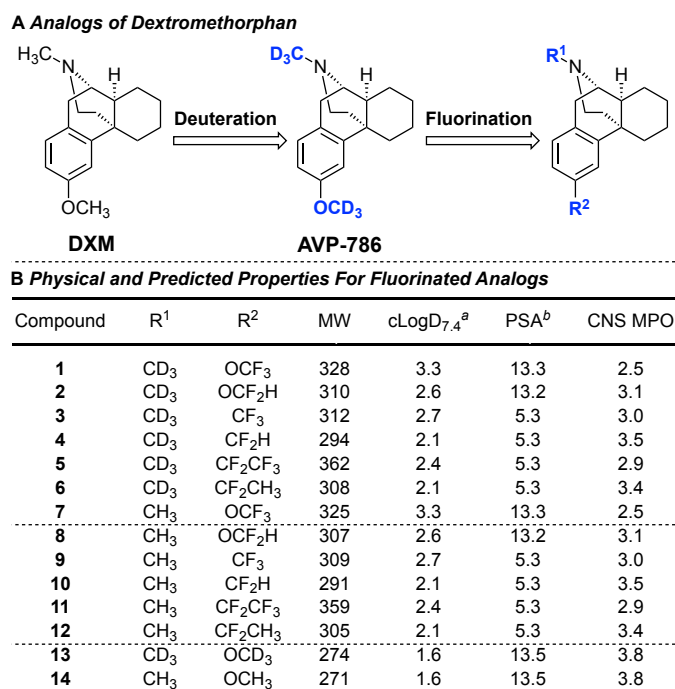


Considering metabolically labile aryl methyl ethers, replacement of the weak C–H bonds with stronger C–D bonds is increasing in popularity (Figure 1B).^{6–8} According to this strategy, the stronger C–D bond dissociation energy (105 kcal/mol for C–D vs. 103 kcal/mol for C–H) slows the initial rate-limiting C–X homolytic cleavage and can marginally improve pharmacokinetic profiles, as demonstrated in the case of dextromethorphan (DXM, Figure 1C),⁹ a cough suppressant that acts via agonism of the σ_1 receptor and has measurable inhibitory activity of the serotonin reuptake transporter (SERT). Specifically, DXM bears an aryl-methyl ether that undergoes facile O-dealkylation by CYP2D6 to reveal a phenolic metabolite, dextrorphan (DXO).^{10,11} Upon consumption of DXM in excessive quantities, the metabolite, DXO, antagonizes the NMDA receptor, which causes dissociative hallucinations. Because of this adverse effect and the ease of acquisition, 5–6% of adults have reported recreational use in their lifetime.^{12–14} In an effort to block metabolism, the hexadeuterated variant of DXM, AVP-786, is currently in clinical trials for several CNS related disorders (Figure 2A),^{9,10,15–17} though the incorporation of deuterium only marginally increases *in vivo* metabolic stability. In fact, to achieve therapeutically relevant *in vivo* pharmacokinetic profiles, AVP-786 still requires co-administration with quinidine,^{9–11,18} a pan P-450 inhibitor with many clinically relevant drug interactions.¹⁹ Thus, to reduce CNS-related adverse effects and improve metabolic profiles, a need remains for a series of DXM analogs with decreased metabolic liabilities as well as minimal NMDA affinity.

As a complementary strategy, fluorination remains essential for perturbing a molecule's physicochemical and biophysical properties that influence distribution, metabolism and pharmacokinetic profiles, while many times retaining or improving the molecule's pharmacodynamic profiles.^{20–22} Considering DXM, we envisioned that the replacement of the aryl methyl ether with a metabolically stable fluoroalkyl ether or ethermimetic might stabilize this labile group, inhibit formation of the phenolic metabolite, and provide an overall improved pharmacokinetic profile, thus removing the need to co-administer the drug with a P-450 inhibitor. Further, minimizing metabolism by CYP2D6 might also minimize pharmacokinetic variability due to differences in patient genotype expression. Such a series of

fluorinated analog series included both electronic and dipole mimics, and bioisosteres, including Ar–OCF₃, –OCF₂H, –CF₃, –CF₂H, –CF₂CF₃, and –CF₂CH₃ (Figure 2A, B), which might minimize changes to the overall pharmacodynamic profile of DXM. However, by minimizing O-dealkylation, the secondary N-dealkylation pathway²³ might become relevant. Knowing that NCH₃ → NCD₃ strategy was taken into the clinic with AVP-786,^{9,10,15–17} we chose to investigate both NCH₃ and NCD₃ variants of the fluoroalkyl analogs.

Figure 2: (A) Design of Fluorinated DXM Analogs. (B) Computed Properties of Analogs.



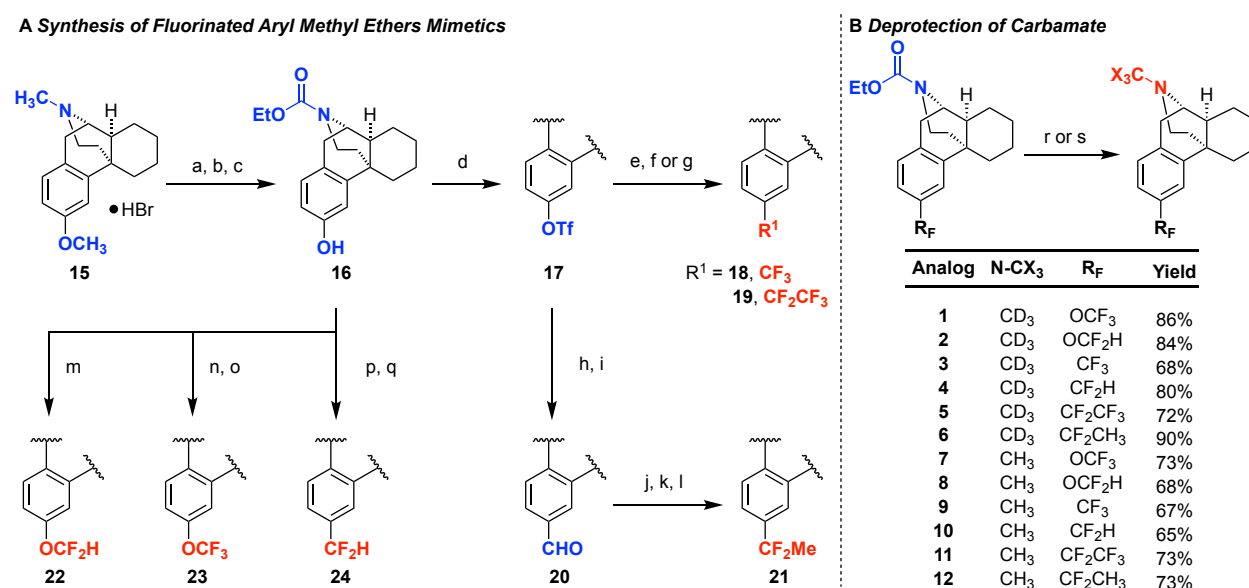
^a Parameters were calculated using MarvinSketch release 20.10 ^b Parameters were calculated using Schrodinger release 2020-1: QikProp. DXM: Dextromethorphan; MW: Molecular Weight; PSA: Polar Surface Area; CNS MPO: Central Nervous System Multiparameter Optimization.

Results and Discussion

In silico analysis indicated that relative to DXM (**14**), fluoroalkyl analogs **1–12** possess higher molecular weights ($\Delta = 20–91$) and cLogD_{7,4} values ($\Delta = 0.5–1.7$); however, these metrics remain in desirable ranges for CNS targeted therapeutics (Figure 2). Additionally, though the removal of oxygen from

several of the analogs reduced the polar surface area (PSA), the overall change was minor. Further, while the inductive effects of fluorinated functional groups can lower the basicity of aliphatic amines, in this case, the fluorinated substructures remained sufficiently distal to not alter the amine's calculated pKa with all analogs in the range of 9.8–9.9. Overall, the calculated central nervous system multiparameter optimization (CNS MPO)^{24,25} scores suggested that the analogs would likely enter the CNS.

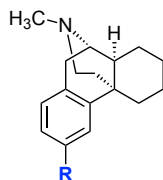
Scheme 1: Synthesis of Fluorinated DXM Analogs.



^a Reagents and conditions: (a) (1) NH₄OH, CHCl₃, rt, 5 min; (2) acetyl chloride, K₂CO₃, DCE, 70 °C, 4 h; (3) MeOH, 70 °C, 30 min; (b) ethyl chloroformate, NEt₃, CHCl₃, 0 to 70 °C, 6 h; (c) BBr₃ (1.0 M in DCM), DCM, 0 °C to rt, 1 h, 87% over 3 steps; (d) Tf₂O, Pyridine, DCM, 0 °C to rt, 1 h, 97%; (e) (Bpin)₂, KOAc, dppf, Pd(dppf)Cl₂, 1,4-dioxane, 80 °C, 18 h, 68%; (f) (phen)CuCF₃, Air, DMF, 50 °C, 18 h, 53%; (g) (phen)CuCF₂CF₃, Air, DMF, 50 °C, 18 h, 43%; (h) tributyl(vinyl)tin, Pd(PPh₃)₄, LiCl, BHT, 1,4-dioxane, 110 °C, 3 h; (i) OsO₄, NaIO₄, THF:H₂O, rt, 1.5 h, 50% over 2 steps; (j) MeMgBr (3.0 M in Et₂O), THF, 0 °C to rt, 2 h; (k) Dess-Martin periodinane, NaHCO₃, DCM, 0 °C to rt, 2 h; (l) bis(2-methoxyethyl)aminosulfur trifluoride (50 wt % in PhMe), 85 °C, 18 h, 30% over 3 steps; (m) KOH, diethyl(bromodifluoromethyl)phosphonate, H₂O:MeCN, 0 °C to rt, 1 h, 56%; (n) NaH, CS₂, MeI, DMF, 0 °C to rt, 16 h; (o) Fluolead, SbCl₃, CH₂Cl₂, 0 to 65 °C, 20 h, 47% over 2 steps; (p) Perfluoro-1-

butanesulfonyl fluoride, NEt₃, DCM, -78 °C to rt, 18 h; (q) TMSCF₂H, Pd(dba)₂, dppf, [SIPr]AgCl, NaO^tBu, PhMe, 110 °C, 18 h, 44% over 2 steps; (r) LiAlH₄, THF, 0 °C to rt, 16 h; (s) LiAlD₄, THF, 0 °C to rt, 16 h.

The fluorinated analogs were synthesized through late-stage functionalization of commercially available DXM•HBr salt, according to our recently published strategy.²⁶ In brief, the basic amine was dealkylated and protected as a carbonate prior to dealkylation of the aryl-methyl ether to reveal phenol **16**.^{9,26} Phenol **16** was triflated, converted to a boronic ester, and subjected to Cu-based perfluoroalkylating reagents to generate CF₃ and CF₂CF₃-derived derivatives (**18** and **19**). Triflate **17** was also coupled with Bu₃Sn(vinyl) to afford corresponding styrene, which was oxidatively cleaved to afford the aldehyde, alkylated with MeMgBr, and oxidized to the corresponding ketone before deoxyfluorination delivered CF₂Me derivative **21**. Phenol **16** was also converted to fluoroalkylether derivatives by (a) reacting with a difluorocarbene surrogate to directly generate OCF₂H derivative **22**, and by (b) conversion to a methyl xanthate prior to oxidative desulfurization-fluorination to furnish OCF₃ intermediate **23**. Finally, phenol **16** was converted to a nonaflate and cross-coupled to deliver CF₂H analog **24**. At this stage, the use of a carbamate protecting group enabled late-stage deprotection/reduction with LiAlH₄ or LiAlD₄ to afford the target analogs **1–12** (Scheme 1).^{9,26}

Table 1: Pharmacodynamic Evaluation of DXM, DXO and Fluorinated Analogs.

Compound	R	K_i (nM) ^a						IC_{50} (nM) ^c		(% Inhib. at 10 μ M) hERG ^d
		σ_1	σ_2	NMDA	SERT	NET	Other Targets ^b	SERT	NET	
14	OCH ₃	73	862	624	18	>10,000	5,242	56	> 10,000	0.1
DXO (15)	OH	118	>10,000	486	401	>340	240	-	-	-
7	OCF ₃	757	833	>10,000	48	>10,000	2,004	31	> 10,000	6.1
8	OCF ₂ H	568	1,281	>10,000	186	>10,000	6,200	55	> 10,000	34.9
9	CF ₃	813	885	>10,000	125	>10,000	>10,000	60	1039	5.1
10	CF ₂ H	145	353	>10,000	51	35	832	24	944	12.0
11	CF ₂ CF ₃	>10,000	1,404	>10,000	>10,000	>10,000	1,161	-	-	-
12	CF ₂ CH ₃	675	826	>10,000	301	>10,000	9,427	-	-	-

^a K_i values were determined by radioligand displacement (see SI for details).²⁷ ^b Represents the lowest K_i for the 43 non-listed targets including dopamine reuptake transporter and 5-HT, acetylcholine, opioid, GABA, histamine, and adrenergic receptors (see SI for full list). ^c IC_{50} was determined by inhibition of substrate transport (see SI for details).²⁷ ^d hERG inhibition was determined by single point inhibition at 10 μ M. Value represents % inhibition.²⁸

To evaluate changes in pharmacodynamic profile, DXM (**14**), DXO (**15**), and analogs **7–12** were screened against a panel of 48 CNS targets through the National Institute of Mental Health Psychoactive Drug Screening Program (NIMH PDSP, Table 1, See SI for additional data).²⁹ Deuterated analogs **1–6** and **13** were not evaluated, as receptor binding is not typically affected by deuteration of a ligand.⁶ Overall, the fluoroalkyl analogs maintained similar profiles relative to DXM, with the benefit of ablating NMDA binding. Pharmacological characterization was conducted according to NIMH PDSP protocols, in which primary screening involved displacement of radiotracers at a single concentration (10 μ M) with hits being defined as >50% displacement. Hits were validated by generating 10-point titration curves from the same radioligand displacement assays to establish binding affinities (Table 1, See SI for primary screening and additional data). Fluorinated analogs **7–12** were moderately selective and demonstrated bound to three conserved targets (σ_1 , σ_2 , and SERT) with sub μ M affinities. No other sub- μ M targets were identified,

with the exception of **10**, which potently bound to NET (35 nM). Relative to DXM (**14**), fluorinated analogs displayed slightly weaker affinity for the σ 1 receptor (**7 – 12**; 145 – >10,000 nM) and maintained modest affinity for the σ 2 receptor (**7 – 12**; 353 – 1,404 nM; Table 1). While binding to σ 1 and σ 2 was anticipated, the high affinity to SERT and NET merited additional assessment to validate functional effects (Table 1). Compounds **7–10** and **14** inhibited SERT with potencies of 24–60 nM, which is comparable to clinically employed SERT inhibitors in the same assay (e.g. fluoxetine IC₅₀ = 36 nM). However, binding to NET only translated to modest inhibition of functional activity (>944 nM). Importantly, analogs **7–12** met our goals of improving off-target profile having less than 50% inhibition of hERG at 10 μ M and no appreciable binding at the NMDA receptor (**7 – 12**; >10,000 nM) relative to DXM (624 nM) and DXO (486 nM). In summary, relative to DXM, the fluoroalkyl analogs maintained SERT inhibitory activity, minimal affinity to the σ 1 and NMDA receptors, and an overall clean CNS profile. Further, this selective profile contrasts that of many approved SERT inhibitors (e.g. sertraline, paroxetine, and escitalopram) that also interact at multiple monoamine transporters and centrally localized receptors.^{30,31}

Table 2: *In Vitro* Solubility and Pharmacokinetic Parameters of DXM, DXO, and Fluorinated Analogs.

Compound	R ¹	R ²	HLM CL (mL/min/kg)	T _{1/2} (min)	MDCK-mdr1 (% Basal)	Solubility _{7.4} (μ M)	Solubility _{3.0} (μ M)	CYP2D6 Metabolism (% remaining after 1 h)	CYP3A4 Metabolism (% remaining after 1 h)
1	CD ₃	OCF ₃	7.81	160	44 ± 3	100 ± 8	86 ± 10	65.3 ± 1	100 ± 15
2	CD ₃	OCF ₂ H	13.2	94.8	55 ± 3	101 ± 5	83 ± 4	-	-
3	CD ₃	CF ₃	15.4	80.7	47 ± 1	95 ± 2	70 ± 5	-	-
4	CD ₃	CF ₂ H	10.2	122	55 ± 1	94 ± 4	70 ± 8	81.3 ± 9	100 ± 6
5	CD ₃	CF ₂ CF ₃	10	124	31 ± 0.3	82 ± 3	70 ± 3	-	-
6	CD ₃	CF ₂ CH ₃	5.39	232	46 ± 2	95 ± 1	67 ± 8	-	-
7	CH ₃	OCF ₃	5.66	220	-	-	-	-	-
8	CH ₃	OCF ₂ H	4.94	253	-	-	-	-	-
9	CH ₃	CF ₃	6.48	192	-	-	-	-	-
10	CH ₃	CF ₂ H	5.13	243	-	-	-	-	-
11	CH ₃	CF ₂ CF ₃	14.4	86.8	-	-	-	-	-
12	CH ₃	CF ₂ CH ₃	8.42	148	-	-	-	-	-
13	CD ₃	OCD ₃	4.72	264	42 ± 1	112 ± 1	95.5 ± 3	14.5 ± 1	100 ± 2
14	CH ₃	OCH ₃	6.09	205	-	-	-	-	-

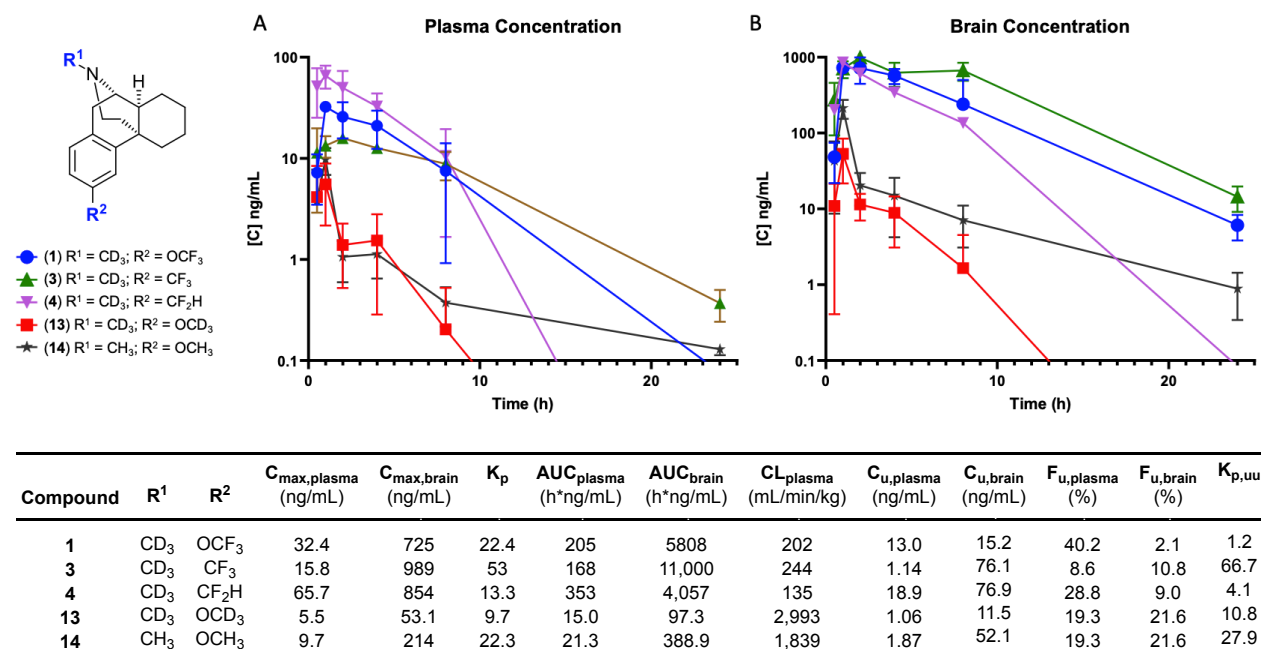
^aA 10 μ M solution of the tested analog was incubated with HLM at a protein concentration of 0.5 mg/mL.

^bA 10 μ M solution of the tested analog was added to the apical side of a transwell plate lined with MDCK-mdr1 cells and incubated for 1.5 h. ^cA 100 μ M solution of the tested analog at a pH of 3.0 or 7.4 was added

to a 0.4 μm multiscreen solubility plate and shaken for 1.5 h before filtering. ^dA 10 μM solution of the tested analog was incubated with 20 pmol/mL of recombinant CYP2D6 or CYP3A4 for 60 min.

Overall, the fluorinated analogs displayed similar physicochemical properties to those of DXM. Specifically, the analogs maintained high aqueous solubility in both physiological and acidic media (66.5 – 112 μM ; Table 2). Despite elevated $\text{clogD}_{7.4}$ values, the fluorinated analogs were not subject to increased transport by P-glycoproteins and passively permeated MDCK-mdr1 cell monolayers. The incorporation of fluorine did not appreciably improve the *in vitro* human liver microsome (HLM) clearance values (**1** – **12**, 4.94 – 15.4 mL/min/kg) relative to DXM (**14**, 6.09 mL/min/kg) and AVP-786 (**13**, 4.72 mL/min/kg). Nonetheless, to further pursue the metabolic hypothesis that replacement of the Ar-OMe group with fluoroalkyl analogs would improve metabolic stability, a subset of molecules (**1**, **4**, and **13**) was incubated with CYP 2D6 and 3A4 isozymes (Table 2). In these isoform-specific assays, the combined incorporation of deuterium and fluorine inhibited transformation by CYP3A4, which generally promotes N-dealkylation reactions of basic amines; however, the fluorinated analogs displayed decreased CYP2D6-dependent metabolism. Based on pharmacodynamic profiles and the conflicting HLM and isoform-specific P450 data, fluoroalkyl analogs **1**, **3**, and **4** were selected for *in vivo* PK analysis.

Figure 3: (A) Plasma and Brain Exposure of Select Compounds (2.5 mg/kg) in SD rats. (B) PK Parameters Derived from *In Vivo* and *In Vitro* Compartmental Studies.



^aCompound was dosed as a solution 0.5% sodium carboxymethylcellulose with 1% NMP and 0.3% Tween 80 at 2.5 mg/kg p.o. ^b20 μ M of compound was incubated with diluted plasma (1:30) and binding was measured by ¹H NMR. ^cA 5 μ M solution of the tested compounds was added to a transwell plate containing SD rat brain homogenate and incubated for 4 h.

To measure *in vivo* distribution and pharmacokinetic properties, a rat PK experiment was conducted for **1**, **3**, and **4** including DXM (**14**) and AVP-786 (**13**) for comparison (Figure 3). This assay exploited a cassette dosing strategy in which compounds were administered 2.5 mg/kg orally (P.O.). Relative to DXM, the tested fluorinated analogs reached higher C_{max} and AUC_{total} in both plasma (C_{max,plasma} = 15.8 – 65.7; AUC_{plasma} = 168 – 353) and brain (C_{max,brain} = 725 – 989; AUC_{brain} = 4,057 – 11,000) than DXM (C_{max,plasma} = 9.7; C_{max,brain} = 214; AUC_{plasma} = 21.3; AUC_{brain} = 388.9). Notably, *in vivo* clearance was drastically reduced for fluorinated analogs (135 – 244 mL/min/kg) relative to DXM (1,839 mL/min/kg) and AVP-786 (2,993 mL/min/kg). Further, the deuterated analogs **1**, **4**, and **13**, have similar *in vivo* stability to their protiated analogs **7**, **10**, and **14** respectively (Figure S1). This improved stability and PK data could

presumably be explained by increased plasma protein binding, though the fluoroalkyl analogs display only moderate plasma binding values ($F_{u,plasma}$: 8.6 – 40.2%). Thus, the intrinsically low reactivity of the fluorinated functional groups toward hepatic metabolism, as opposed to protein binding, might best explain the improved stability profiles of **1**, **3**, and **4**.

Further, the tested analogs and DXM demonstrated high partitioning into the CNS ($K_p = 9.6 – 63$). This partitioning could potentially derive from the greater lipophilicity of the fluorinated analogs that localizes the drugs into brain tissue that contains roughly 20-fold more lipid than plasma.³² To account for the differences in lipid content, free drug concentrations were determined by measuring the binding of the compounds to both plasma and brain homogenate. Notably, the fluoroalkyl analogs displayed increased binding to brain homogenate ($F_{u,brain}$: 2.1 – 10.8%) relative to DXM ($F_{u,brain} = 21.6$). Further, both DXM and the CF_3 and CF_2H analogs (**3–4**) displayed high $K_{p,uu}$ (4.1 – 66.7), which suggested that active transport, not passive tissue partitioning, appropriately explains the higher concentrations reached in the CNS.³² However, with a $K_{p,uu}$ value nearing 1, the equilibrium of OCF_3 analog (**1**) is not appreciably influenced by active transport and is better rationalized as the outcome of passive diffusion.³²

Conclusion

The evaluation of fluorinated aryl-methyl ether mimetics is critical improving the *in vivo* stability of this labile functional group. Through late-stage modification of a natural product-like scaffold, this study delivered fluoroalkyl analogs that retained a clean CNS pharmacological profile, while minimizing *in vivo* clearance and increasing CNS exposure relative to the parent compound DXM and the deuterated analog AVP-786. Ultimately, these fluoroalkyl motifs improve drug-like properties of other aryl-methyl ether containing natural products, and this strategy provides a roadmap for late-stage functionalization of other natural product-derived therapeutic candidates.

ASSOCIATED CONTENT

Supporting Information

The Supporting Information is available free of charge at

Copies of HPLC, ¹H, ¹³C{¹H}, ¹⁹F, and ²H NMR spectra for synthesized compounds, radioligand binding data, neurotransmitter transporter data, hERG inhibition data, aqueous solubility data, HLM stability data, human cytochrome P450 metabolism data, MDCK-mdr1 permeability data, *in vivo* pk data, plasma protein binding NMR data, and brain tissue binding

AUTHOR INFORMATION

Corresponding Author

Ryan A. Altman – Department of Medicinal Chemistry and Molecular Pharmacology and Department of Chemistry
Purdue University, West Lafayette, IN, 47906, United States;
orcid.org/0000-0002-8724-1098; Email: raaltman@purdue.edu

Present Address

Jacob P. Sorrentino – Department of Medicinal Chemistry, The University of Kansas, Lawrence, Kansas 66045, United States;
orcid.org/0000-0001-5071-5379

Author Contributions

The manuscript was written through contributions of all authors. All authors have given approval to the final version of the manuscript.

Funding Sources

We thank the National Institutes of Health (R35 GM124661). NMR Instrumentation was provided by NIH Shared Instrumentation Grants S10OD016360 and S10RR024664; NSF Major Research Instrumentation Grants 9977422, 1625923, and 0320648; and NIH Center Grant P20GM103418. *K_i* determinations, receptor binding profiles, agonist and antagonist functional data and hERG data was generously provided by the National Institute of Mental Health's Psychoactive Drug Screening Program, Contract # HHSN-271-2018-00023-C (NIMH PDSP).

Notes

The authors declare no competing financial interest.

ACKNOWLEDGMENTS

We thank Dr. Minli Xing for experimental guidance for evaluating compound plasma protein binding by NMR, and Dr. Brett Ambler for early synthetic efforts on this project, and helpful discussions about the manuscript. The NIMH PDSP is Directed by Bryan L. Roth MD, PhD at the University of North Carolina at Chapel Hill and Project Officer Jamie Driscoll at NIMH, Bethesda MD, USA.

ABBREVIATIONS

BHT, 2,6-bis(1,1-dimethylethyl)-4-methylphenol; (Bpin)₂, bis(pinacolato)diboron; CNS MPO, central nervous system multiparameter optimization; dppf, 1,1'-Bis(diphenylphosphino)ferrocene; DXO, dextroprphan; DXM, dextromethorphan; GABA, γ -aminobutyric acid; HLM, human liver microsome; MDCK, Madin Darby canine kidney; NET, norepinephrine transporter; NMDA; N-methyl-D-aspartate; PDSP, Psychoactive Drug Screening Program; phen, phenanthroline; PSA, polar surface area; SD, Sprague Dawley; SERT, serotonin reuptake transporter.

REFERENCES

- (1) Springob, K.; Kutchan, T. *Introduction to Different Classes of Natural Products. In Plant-Derived*

- Natural Products Synthesis, Function, and Application*; Osbourn, A., Lanzotti, V., Eds.; Springer. <https://doi.org/10.1007/978-0-387-85498-4>.
- (2) Teponno, R.; Kusari, S.; Spittler, M. Recent Advances in Research on Lignans and Neolignans. *Nat. Prod. Rep* **2016**, *33*, 1044–1092. <https://doi.org/10.1039/c6np00021e>.
 - (3) Smith, H. S. Opioid Metabolism. *Mayo Clin Proc.* **2009**, *84*, 613–624.
 - (4) Zhou, S.; Liu, J.; Chowbay, B.; Zhou, S.; Liu, J.; Chowbay, B. Polymorphism of Human Cytochrome P450 Enzymes and Its Clinical Impact. *Drug Metab. Rev.* **2009**, *41*, 89–295. <https://doi.org/10.1080/03602530902843483>.
 - (5) Kerns, E.; Di, L. *Metabolic Stability. In Drug-like Properties: Concepts, Structures Design and Methods, from ADME to Toxicity Optimization*; Elsevier, 2008.
 - (6) Pirali, T.; Serafini, M.; Cargnin, S.; Genazzani, A. A. Applications of Deuterium in Medicinal Chemistry. *J. Med. Chem.* **2019**, *62* (11), 5276–5297. <https://doi.org/10.1021/acs.jmedchem.8b01808>.
 - (7) Stepan, A. F.; Mascitti, V.; Beaumont, K.; Kalgutkar, A. S. Metabolism-Guided Drug Design. *Medchemcomm* **2013**, *4*, 631–652. <https://doi.org/10.1039/c2md20317k>.
 - (8) Sharma, R.; Strelevitz, T. J.; Gao, H.; Clark, A. J.; Schildknecht, K.; Obach, R. S.; Ripp, S. L.; Spracklin, D. K.; Tremaine, L. M.; Vaz, A. D. N. Deuterium Isotope Effects on Drug Pharmacokinetics. I. System-Dependent Effects of Specific Deuteration with Aldehyde Oxidase Cleared Drugs. *Drug Metab. Dispos.* **2012**, *40* (3), 625–634. <https://doi.org/10.1124/dmd.111.042770>.
 - (9) Tung, R. Preparation of Morphinan Derivatives for Therapeutic Use in Pharmaceutical Compositions for the Treatment of Neuropathic Pain. WO 2008/137474 A1, 2008.
 - (10) Taylor, C. P.; Traynelis, S. F.; Siffert, J.; Pope, L. E.; Matsumoto, R. R. Pharmacology & Therapeutics Pharmacology of Dextromethorphan : Relevance to Dextromethorphan / Quinidine (Nuedexta ®) Clinical Use. *Pharmacol. Ther.* **2016**, *164*, 170–182. <https://doi.org/10.1016/j.pharmthera.2016.04.010>.
 - (11) Pope, L. E.; Khalil, M. H.; Berg, J. E. Pharmacokinetics of Dextromethorphan After Single or Multiple Dosing in Combination With Quinidine in Extensive and Poor Metabolizers. *J. Clin. Pharmacol* **2004**, *44*, 1132–1142. <https://doi.org/10.1177/0091270004269521>.
 - (12) Karami, S.; Major, J. M.; Calderon, S.; McAninch, J. K.; Karami, S.; Major, J. M.; Calderon, S.; McAninch, J. K. Trends in Dextromethorphan Cough and Cold Products : 2000 – 2015 National Poison Data System Intentional Abuse Exposure Calls. *Clin. Toxicol.* **2018**, *56* (7), 656–663. <https://doi.org/10.1080/15563650.2017.1416124>.
 - (13) Bryner, J. K.; Wang, U. K.; Hui, J. W.; Bedodo, M.; Macdougall, C.; Anderson, I. B. Dextromethorphan Abuse in Adolescence. *Arch Pediatr Adolesc Med* **2008**, *160* (12), 1217–1222.
 - (14) Wilson, M. D.; Ferguson, R. W.; Mazer, M. E.; Litovitz, T. L.; Wilson, M. D.; Ferguson, R. W.; Mazer, M. E.; Litovitz, T. L.; Wilson, M. D.; Ferguson, R. W.; Mazer, M. E.; Litovitz, T. L. Monitoring Trends in Dextromethorphan Abuse Using the National Poison Data System : 2000 – 2010. *Clin. Toxicol.* **2011**, *49*, 409–415. <https://doi.org/10.3109/15563650.2011.585429>.
 - (15) Vepachedu, S.; Moebius, H.; Besspalov, A. Targeted Drug Rescue with Novel Compositions Comprising Double and/or Triple Agent or Ligand for CYP2D6, 5-HT2A, and/or 5HT2C Receptors, and/or Acetylcholinesterase, Combinations, and Methods Thereof. WO 2018204713,

2018.

- (16) Thomas, A. Combination of Morphinan Compounds and Antidepressant for the Treatment of Pseudobulbar Affect, Neurological Diseases, Intractable and Chronic Pain and Brain Injury. WO 2010062692, 2010.
- (17) Sircar, J.; Kumar, S. Pharmaceutical Compositions Comprising Dextromethorphan Analogs for the Treatment of Neurological Disorders. WO 2008097924, 2008.
- (18) Murrugh, J. W.; Wade, E.; Sayed, S.; Ahle, G.; Kiraly, D. D.; Welch, A.; Collins, K. A.; Soleimani, L.; Iosifescu, D. V.; Charney, D. S. Dextromethorphan / Quinidine Pharmacotherapy in Patients with Treatment Resistant Depression : A Proof of Concept Clinical Trial. *J. Affect. Disord.* **2017**, *218*, 277–283. <https://doi.org/10.1016/j.jad.2017.04.072>.
- (19) Bahar, M. A.; Setiawan, D.; Hak, E.; Wilffert, & B. Pharmacogenetics of Drug–Drug Interaction and Drug–Drug–Gene Interaction: A Systematic Review on CYP2C9, CYP2C19 and CYP2D6. *Pharmacogenomics* **2017**, *18*, 701–739. <https://doi.org/10.2217/pgs-2017-0194>.
- (20) Gillis, E. P.; Eastman, K. J.; Hill, M. D.; Donnelly, D. J.; Meanwell, N. A. Applications of Fluorine in Medicinal Chemistry. *J. Med. Chem.* **2015**, *58* (21), 8315–8359. <https://doi.org/10.1021/acs.jmedchem.5b00258>.
- (21) Meanwell, N. A. Fluorine and Fluorinated Motifs in the Design and Application of Bioisosteres for Drug Design. *J. Med. Chem.* **2018**, *61*, 5822–5880. <https://doi.org/10.1021/acs.jmedchem.7b01788>.
- (22) Johnson, B. M.; Shu, Y.-Z.; Zhuo, X.; Meanwell, N. A. Metabolic and Pharmaceutical Aspects of Fluorinated Compounds. *J. Med. Chem.* **2020**, *63* (12), 6315–6386. <https://doi.org/10.1021/acs.jmedchem.9b01877>.
- (23) Silva, A. R.; Dinis-Oliveira, R. J. Pharmacokinetics and Pharmacodynamics of Dextromethorphan: Clinical and Forensic Aspects. *Drug Metab. Rev.* **2020**, *52* (2), 258–282. <https://doi.org/10.1080/03602532.2020.1758712>.
- (24) Wager, T. T.; Hou, X.; Verhoest, P. R.; Villalobos, A. Moving beyond Rules: The Development of a Central Nervous System Multiparameter Optimization (CNS MPO) Approach to Enable Alignment of Druglike Properties. *ACS Chem. Neurosci.* **2010**, *1* (6), 435–449. <https://doi.org/10.1021/cn100008c>.
- (25) Wager, T. T.; Hou, X.; Verhoest, P. R.; Villalobos, A. Central Nervous System Multiparameter Optimization Desirability: Application in Drug Discovery. *ACS Chem. Neurosci.* **2016**, *7* (6), 767–775. <https://doi.org/10.1021/acschemneuro.6b00029>.
- (26) Sorrentino, J. P.; Ambler, B. R.; Altman, R. A. Late-Stage Conversion of a Metabolically Labile Aryl Methyl Ether-Containing Natural Product to Fluoroalkyl Analogues. *J. Org. Chem.* **2020**, *85* (8), 5416–5427. <https://doi.org/10.1021/acs.joc.0c00125>.
- (27) Besnard, J.; Ruda, G. F.; Setola, V.; Abecassis, K.; Rodriguiz, R. M.; Huang, X.-P.; Norval, S.; Sassano, M. F.; Shin, A. I.; Webster, L. A.; Simeons, F. R. C.; Stojanovski, L.; Prat, A.; Seidah, N. G.; Constam, D. B.; Bickerton, G. R.; Read, K. D.; Wetsel, W. C.; Gilbert, I. H.; Roth, B. L.; Hopkins, A. L. Automated Design of Ligands to Polypharmacological Profiles. *Nature* **2012**, *492* (7428), 215–220. <https://doi.org/10.1038/nature11691>.
- (28) Huang, Xi-Ping; Mangano, Thomas; Hufeisen, Sandy; Setola, Vincent; Roth, B. L. Identification of Human Ether-a-Go-Go Related Gene Modulators by Three Screening Platforms in an Academic Drug-Discovery Setting. *Assay Drug Dev. Technol.* **2010**, *8*, 727–742.

<https://doi.org/10.1089/adt.2010.0331>.

- (29) Roth, B. L. *National Institute of Mental Health Psychoactive Drug Screening Program (NIMH PDSP) Assay Protocol Book Version III*; 2018.
- (30) Owens, M. J.; Knight, D. L.; Nemeroff, C. B. Second-Generation SSRIs: Human Monoamine Transporter Binding Profile of Escitalopram and R-Fluoxetine. *BIOL PSYCHIATRY* **2001**, No. 50, 345–350.
- (31) Hindmarch, I.; Hashimoto, K. Cognition and Depression : The Effects of Fluvoxamine , a Sigma-1 Receptor Agonist , Reconsidered. *Hum. Psychopharmacol Clin Exp* **2010**, No. 25, 193–200. <https://doi.org/10.1002/hup>.
- (32) Rankovic, Z. CNS Drug Design: Balancing Physicochemical Properties for Optimal Brain Exposure. *J. Med. Chem.* **2015**, 58 (6), 2584–2608. <https://doi.org/10.1021/jm501535r>.